The Inclusive Decay $B \to \eta X$

Y. Kubota,[1] M. Lattery,[1] M. Momayezi,[1] J.K. Nelson,[1] S. Patton,[1] R. Poling,[1] V. Savinov,[1] S. Schrenk,[1] R. Wang,[1] M.S. Alam,[2] I.J. Kim,[2] Z. Ling,[2] A.H. Mahmood,[2] J.J. O'Neill,[2] H. Severini,[2] C.R. Sun,[2] F. Wappler,[2] G. Crawford,[3] C. M. Daubenmier,[3] R. Fulton,[3] D. Fujino,[3] K.K. Gan,[3] K. Honscheid,[3] H. Kagan,[3] R. Kass,[3] J. Lee,[3] M. Sung,[3] C. White,[3] A. Wolf,[3] M.M. Zoeller,[3] F. Butler,[4] X. Fu,[4] B. Nemati,[4] W.R. Ross,[4] P. Skubic,[4] M. Wood,[4] M. Bishai,[5] J. Fast,[5] E. Gerndt,[5] J.W. Hinson,[5] R.L. McIlwain,[5] T. Miao,[5] D.H. Miller,[5] M. Modesitt,[5] D. Payne,[5] E.I. Shibata,[5] I.P.J. Shipsey,[5] P.N. Wang,[5] M. Battle,[6] J. Ernst,[6] L. Gibbons,[6] Y. Kwon,[6] S. Roberts,[6] E.H. Thorndike,[6] C.H. Wang,[6] J. Dominick,[7] M. Lambrecht,[7] S. Sanghera,[7] V. Shelkov,[7] T. Skwarnicki,[7] R. Stroynowski,[7] I. Volobouev,[7] G. Wei,[7] P. Zadorozhny,[7] M. Artuso,[8] M. Gao,[8] M. Goldberg,[8] D. He,[8] N. Horwitz,[8] G.C. Moneti,[8] R. Mountain,[8] F. Muheim,[8] Y. Mukhin,[8] S. Playfer,[8] Y. Rozen,[8] S. Stone,[8] X. Xing,[8] G. Zhu,[8] J. Bartelt,[9] S.E. Csorna,[9] Z. Egyed,[9] V. Jain,[9] D. Gibaut,[10] K. Kinoshita,[10] P. Pomianowski,[10] B. Barish,[11] M. Chadha,[11] S. Chan,[11] D.F. Cowen,[11] G. Eigen,[11] J.S. Miller,[11] C. O'Grady,[11] J. Urheim,[11] A.J. Weinstein,[11] M. Athanas,[12] W. Brower,[12] G. Masek,[12] H.P. Paar,[12] J. Gronberg,[13] C.M. Korte,[13] R. Kutschke,[13] S. Menary,[13] R.J. Morrison,[13] S. Nakanishi,[13] H.N. Nelson,[13] T.K. Nelson,[13] C. Qiao,[13] J.D. Richman,[13] A. Ryd,[13] D. Sperka,[13] H. Tajima,[13] M.S. Witherell,[13] R. Balest,[14] K. Cho,[14] W.T. Ford,[14] D.R. Johnson,[14] K. Lingel,[14] M. Lohner,[14] P. Rankin,[14] J.G. Smith,[14] J.P. Alexander,[15] C. Bebek,[15] K. Berkelman,[15] K. Bloom,[15] T.E. Browder,[15*] D.G. Cassel,[15] H.A. Cho,[15] D.M. Coffman,[15] D.S. Crowcroft,[15] P.S. Drell,[15] D.J. Dumas,[15] R. Ehrlich,[15] P. Gaidarev,[15] M. Garcia-Sciveres,[15] B. Geiser,[15] B. Gittelman,[15] S.W. Gray,[15] D.L. Hartill,[15] B.K. Heltsley,[15] S. Henderson,[15] C.D. Jones,[15] S.L. Jones,[15] J. Kandaswamy,[15] N. Katayama,[15] P.C. Kim,[15] D.L. Kreinick,[15] G.S. Ludwig,[15] J. Masui,[15] J. Mevissen,[15] N.B. Mistry,[15] C.R. Ng,[15] E. Nordberg,[15] J.R. Patterson,[15] D. Peterson,[15] D. Riley,[15] S. Salman,[15] M. Sapper,[15] F. Würthwein,[15] P. Avery,[16] A. Freyberger,[16] J. Rodriguez,[16] S. Yang,[16] J. Yelton,[16] D. Cinabro,[17] T. Liu,[17] M. Saulnier,[17] R. Wilson,[17] H. Yamamoto,[17] T. Bergfeld,[18] B.I. Eisenstein,[18] G. Gollin,[18] B. Ong,[18] M. Palmer,[18] M. Selen,[18] J. J. Thaler,[18] K.W. Edwards,[19] M. Ogg,[19] A. Bellerive,[20] D.I. Britton,[20] E.R.F. Hyatt,[20] D.B. MacFarlane,[20] P.M. Patel,[20] B. Spaan,[20] A.J. Sadoff,[21] R. Ammar,[22] P. Baringer,[22] A. Bean,[22] D. Besson,[22] D. Coppage,[22] N. Copty,[22] R. Davis,[22] N. Hancock,[22] M. Kelly,[22] S. Kotov,[22] I. Kravchenko,[22] N. Kwak,[22] and H. Lam[22]

(CLEO Collaboration)

[1] *University of Minnesota, Minneapolis, Minnesota 55455*

[2] *State University of New York at Albany, Albany, New York 12222*

[3] *Ohio State University, Columbus, Ohio, 43210*

[4] *University of Oklahoma, Norman, Oklahoma 73019*

[5] *Purdue University, West Lafayette, Indiana 47907*

[6] *University of Rochester, Rochester, New York 14627*

[7] *Southern Methodist University, Dallas, Texas 75275*

[8] *Syracuse University, Syracuse, New York 13244*

[9] *Vanderbilt University, Nashville, Tennessee 37235*

[10] *Virginia Polytechnic Institute and State University, Blacksburg, Virginia, 24061*

[11] *California Institute of Technology, Pasadena, California 91125*

[12] *University of California, San Diego, La Jolla, California 92093*

[13] *University of California, Santa Barbara, California 93106*

[14] *University of Colorado, Boulder, Colorado 80309-0390*

[15] *Cornell University, Ithaca, New York 14853*

[16] *University of Florida, Gainesville, Florida 32611*

[17] *Harvard University, Cambridge, Massachusetts 02138*

[18] *University of Illinois, Champaign-Urbana, Illinois, 61801*

[19] *Carleton University, Ottawa, Ontario K1S 5B6 and the Institute of Particle Physics, Canada*

[20] *McGill University, Montréal, Québec H3A 2T8 and the Institute of Particle Physics, Canada*

[21] *Ithaca College, Ithaca, New York 14850*

[22] *University of Kansas, Lawrence, Kansas 66045*

Using data samples taken at the $\Upsilon(4S)$ resonance and nearby continuum e^+e^- annihilation with the CLEO II detector at CESR, we have measured the inclusive branching fraction $\mathcal{B}(B \to \eta X)$=(17.6±1.1±1.2)%, and the momentum distribution of the η mesons from B meson decay. The

[*] Permanent address: University of Hawaii at Manoa

η yield cannot be explained as arising solely from the decay of intermediate charmed mesons.

PACS number(s): 13.25.Hw, 13.65.+i

Little is known about the inclusive production of light mesons from the decays of B mesons. In this paper we report a measurement of the $B \to \eta X$ branching fraction and the momentum spectrum of η mesons from B meson decay.

The data used in this analysis were recorded with the CLEO-II detector [1] at the Cornell Electron Storage Ring. An integrated luminosity of 927 pb^{-1} was accumulated at the $\Upsilon(4S)$ resonance and a further 416 pb^{-1}, denoted as 'continuum' data, was collected at energies just below that resonance. To eliminate events not consistent with having come from $e^+e^- \to q\bar{q}$, we require that each event has at least 3 charged tracks originating from the interaction region and a visible energy of at least 15% of the total center of mass energy. Since B mesons produced in $\Upsilon(4S)$ are nearly at rest, $B\bar{B}$ events have a spherical topology while the background continuum production of light quark pairs tends to produce two jets. To suppress non-$B\bar{B}$ events, we require that the event shape parameter R2, the ratio of second and zeroth Fox Wolfram moments [2], be less than 0.3.

We measure the η yield in each 100 MeV interval in momentum for both the $\Upsilon(4S)$ and the continuum. The yield from B meson decays is determined by subtracting the number measured in the continuum, scaled to account for the relative on-/off-resonance luminosities and the s^2 dependence of the continuum cross-section, from that found in the on-resonance data and then correcting for efficiencies.

We use the $\eta \to \gamma\gamma$ decay channel since it has a large branching fraction, 38.9% [3], and the CLEO II detector has excellent photon detection with its CsI crystal electromagnetic calorimeter. We detect photons only in the the barrel region of the calorimeter, defined by $|\cos\theta| < 0.71$ where θ is the angle of the shower with respect to beamline. The photon energy resolution for the barrel region is $\delta E/E(\%) = 0.35/E^{3/4} + 1.9 - 0.1E$, where E is in GeV. We require that each photon candidate be found in a single isolated neutral energy cluster with a minimum energy of 10 MeV, and that it have a lateral shower shape consistent with that expected for photons. Combinatoric background tends to preferentially populate asymmetric decays. To suppress this background, we require the decay angle of the photon, defined as the angle between the photon momentum in the $\gamma\gamma$ frame and the $\gamma\gamma$ lab momentum, to have a cosine less than 0.85.

Fig. 1 shows the $\gamma\gamma$ mass spectra from the sum of $\Upsilon(4S)$ and continuum data, without an $R2$ cut, for two momentum intervals: (a) 0.8-0.9 GeV/c and (b) 1.4-1.5 GeV/c. The curves are the result of fitting the data with a function consisting of a polynomial background term and an asymmetric Gaussian (i.e., it has different widths below, σ_A, and above the mean, σ_B) for the signal. The asymmetry comes from the γ energy loss due to crystal rear-end leakage. The spectra from the sum of the continuum and $\Upsilon(4S)$ data without the $R2$ cut are used to determine the parameters for the signal function. We find that the mass is constant as a function of momentum with an average value of 547.0$\pm$0.3 MeV, which is consistent with the world average value 547.45$\pm$0.19 MeV [3]. We fix the η mass in all subsequent fits to 547.0 MeV. The two r.m.s. widths, σ_A and σ_B, have also been derived from the data. These are shown in Fig. 2 (a) and (b) as a function of η momentum. The same r.m.s. widths obtained from Monte Carlo simulation are shown in Fig. 2 (c) and (d). In the low momentum region the data do not determine these widths well due to the large π^0 background. In contrast, the widths found from the Monte Carlo are poorly determined in the high momentum region above 2.0 GeV due to insufficient statistics. In the intermediate region the agreement between data and Monte Carlo is excellent. We have chosen to use the weighted average of the data and Monte Carlo distributions for the variation of these σ's with momentum. In Fig. 2 (e) and (f) we show this average and third order polynomial fits which we use to fix the σ's in our subsequent analysis.

In Fig. 3, the $\gamma\gamma$ invariant mass plot for the η momentum interval 0.8 to 2.0 GeV/c is shown for: (a) $\Upsilon(4S)$ data , (b) continuum data , and (c) $\Upsilon(4S)$ data after scaled continuum subtraction. The number of signal events is derived from (c).

The η detection efficiency as a function of η momentum, found by Monte Carlo simulation, is shown in Fig. 4. The efficiency does not include the $\eta \to \gamma\gamma$ branching fraction. The photon detection efficiency in the barrel calorimeter is about 50%. Hence, the $\eta \to \gamma\gamma$ mode will have a reconstruction efficiency around 25% if the directions of the two γ's are uncorrelated. The efficiency increases at lower momentum, however, due to the nearly complete correlation in the directions of the two γ's, and at higher momentum due to the partial correlation. We fit the data of Fig. 4 with a smooth curve and then use the fitted values to deduce the efficiency corrected rates.

The number of events, the efficiency, and the branching fraction in each momentum interval are listed in Table I. The efficiency corrected η momentum spectrum is shown in Fig. 5. The errors shown are statistical only and include the error from the fit to the efficiency curve.

TABLE I. Numbers of Events

P (GeV)	# of events	ϵ(%)	$\mathcal{B}$(%/GeV)
0.0-0.1	500$\pm$189	39.5	1.7$\pm$0.6
0.1-0.2	810$\pm$416	34.2	3.1$\pm$1.6
0.2-0.3	2519$\pm$1092	30.2	11.1$\pm$4.8
0.3-0.4	4397$\pm$878	27.4	21.3$\pm$4.3
0.4-0.5	3207$\pm$986	25.5	16.7$\pm$5.1
0.5-0.6	3812$\pm$684	24.4	20.7$\pm$3.7
0.6-0.7	3581$\pm$579	23.9	19.9$\pm$3.2
0.7-0.8	3658$\pm$410	24.0	20.2$\pm$2.3

0.8-0.9	2534±339	24.4	13.8±1.8
0.9-1.0	2383±284	25.1	12.6±1.5
1.0-1.1	1672±219	26.0	8.5±1.1
1.1-1.2	1518±188	26.9	7.5±0.9
1.2-1.3	905±161	27.8	4.3±0.8
1.3-1.4	999±138	28.6	4.6± 0.6
1.4-1.5	589±122	29.4	2.7±0.6
1.5-1.6	486±105	30.0	2.2±0.5
1.6-1.7	407±94	30.4	1.8±0.4
1.7-1.8	250±82	30.7	1.1±0.4
1.8-1.9	240±73	30.8	1.0±0.3
1.9-2.0	50±66	30.8	0.2±0.3
2.0-2.1	169±57	30.6	0.7±0.2
2.1-2.2	78±51	30.1	0.3±0.2
2.2-2.3	45±48	30.1	0.2±0.2
2.3-2.4	-76±45	30.1	-0.3±0.2
2.4-2.5	86±39	30.1	0.4±0.2

The total branching fraction is obtained by summing the data from the individual momentum bins. We find $\mathcal{B}(B \to \eta X)=$ (17.6±1.1±1.2)%, where the first error is statistical and the second one is systematic. The major systematic error arises from the uncertainty in the photon detection efficiency. This has been studied by measuring the ratio $\Gamma(\eta \to \pi^0\pi^0\pi^0)/\Gamma(\eta \to \gamma\gamma)$ in our detector and comparing with the PDG vale [3]. We find an uncertainty of ±6%. We estimate the overall systematic error from background parameterization to be ±3%. We have found that the yield is insensitive to the value of the $R2$ cut which is used. [1]

The inclusive B branching fraction to η found here is about a factor of 7 larger than the measured branching fraction to ϕ of (2.3±0.8)% [4]. The processes that could yield a significant amount of η's include D^0, D^+, and D_s^+ decay as well as fragmentation, either of the virtual W^- or between the charm quark and spectator antiquark. We estimate the branching fractions for η production via D^0, D^+ and D_s^+ decay by summing the branching fractions that have been observed to date [3]. These values and the remaining branching fraction of η's from fragmentation are listed in Table II.

TABLE II. Branching Fractions of the Three $B \to \eta X$ Processes

Process	Branching Fraction
$B \to \eta X$	(17.6±1.6)%
$B \to \sum\{D(D^0, D^+) \to \eta\}$	(2.5±0.5)%
$B \to \sum\{D_s \to \eta\}$	(2.8±0.6)%
Difference	(12.3±1.8)%

[1] An $R2$ cut of 0.3 keeps 84% of generic $B\bar{B}$ events and rejects 60% of continuum events.

In conclusion, we measure $\mathcal{B}(B \to \eta X)$=(17.6±1.1±1.2)%. This rate combined with the measured inclusive B to charm rates indicates that charmed meson intermediate states are not the dominant source of η's in B meson decay.

ACKNOWLEDGEMENTS

We gratefully acknowledge the effort of the CESR staff in providing us with excellent luminosity and running conditions. J.P.A., J.R.P., and I.P.J.S. thank the NYI program of the NSF, G.E. thanks the Heisenberg Foundation, I.P.J.S. and T.S. thank the TNRLC, K.K.G., M.S., H.N.N., T.S., and H.Y. thank the OJI program of DOE, J.R.P thanks the A.P. Sloan Foundation, S.M.S. thanks the Islamic Development Bank, and A.W. thanks the Alexander von Humboldt Stiftung for support. This work was supported by the National Science Foundation, the U.S. Dept. of Energy and the Natural Sciences and Engineering Research Council of Canada.

[1] CLEO Collaboration, Y. Kubota et al., Nucl. Inst. and Meth. **66**, A320 (1992).
[2] G. Fox and S. Wolfram, Phys. Rev. Lett. **41**, 1581 (1978).
[3] Particle Data Group, K. Hikasa *et al.*, Phys. Rev. D **45**, Part II (1994).
[4] D. Bortoletto et al., Phys. Rev. Lett. **56**, 800 (1986).

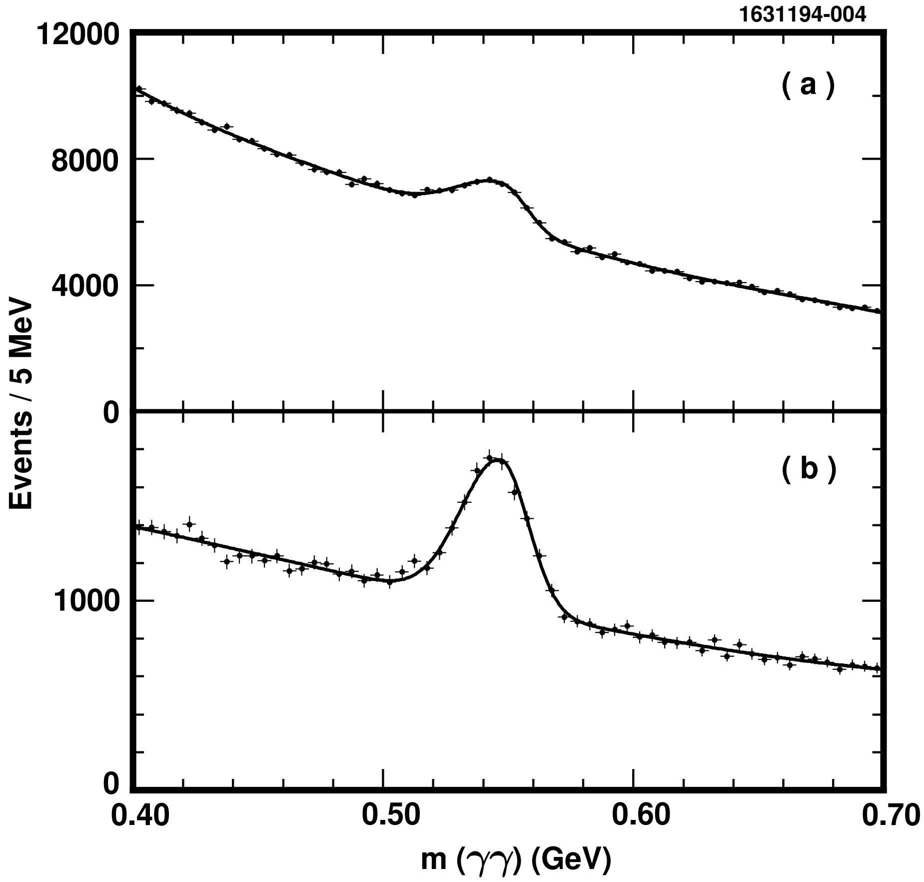

FIG. 1. The $\gamma\gamma$ mass spectrum for the sum of $\Upsilon(4S)$ and continuum data, for the momentum intervals (a) 0.8-0.9 GeV/c and (b) 1.4-1.5 GeV/c.

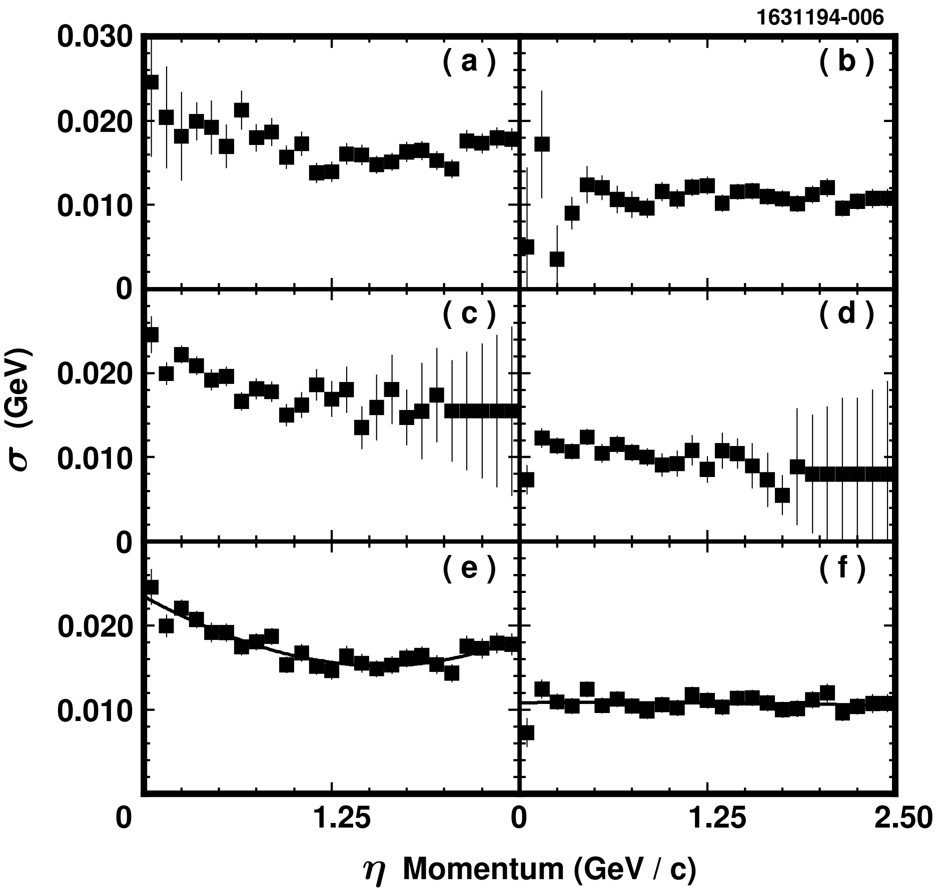

FIG. 2. σ_A and σ_B given as functions of η momenta as determined from data (a) and (b) and Monte Carlo simulation (c) and (d). In (e) and (f) the error weighted average of the data and Monte Carlo is shown with fits to third order polynomial.

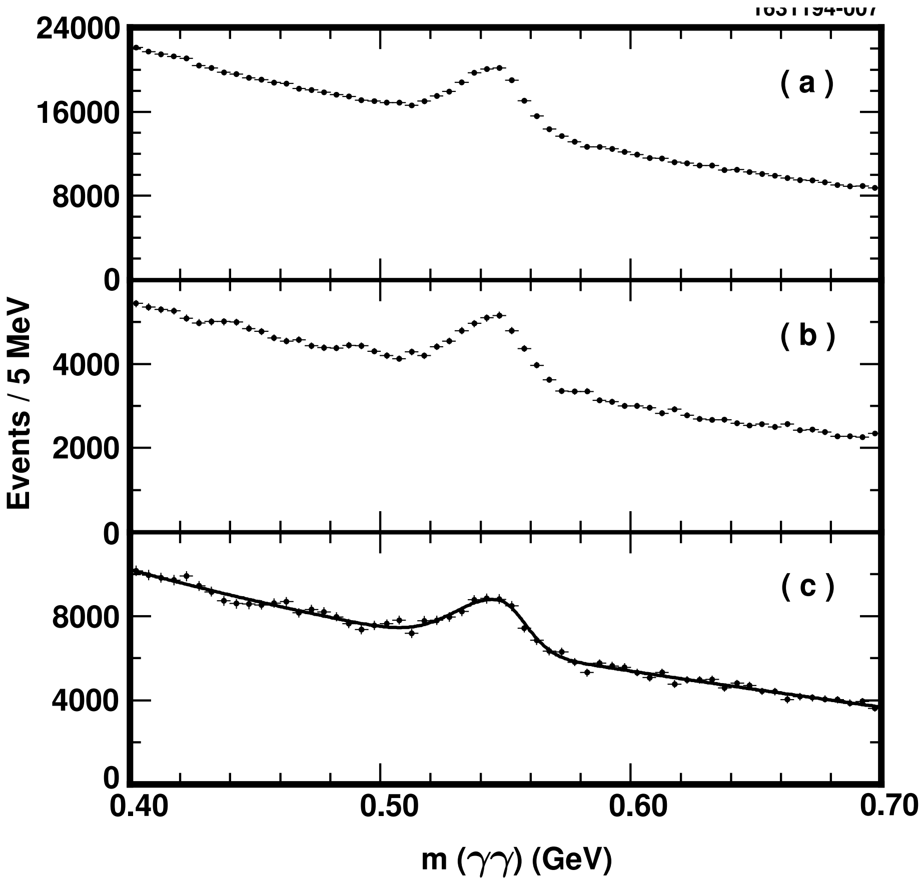

FIG. 3. The $\gamma\gamma$ mass spectra for (a)$\Upsilon(4S)$ data, (b) continuum data, and (c) scaled continuum subtracted. The η momentum interval is 0.8 to 2.0 GeV/c.

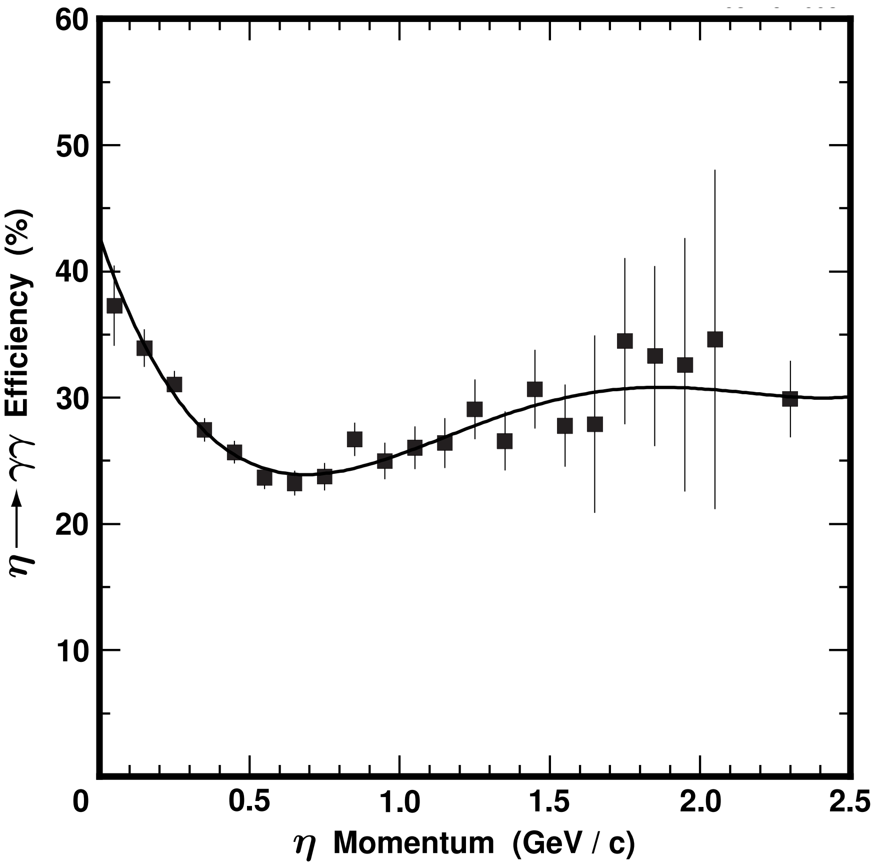

FIG. 4. Monte Carlo generated η efficiency. The curve is a fit to a fourth order polynomial.

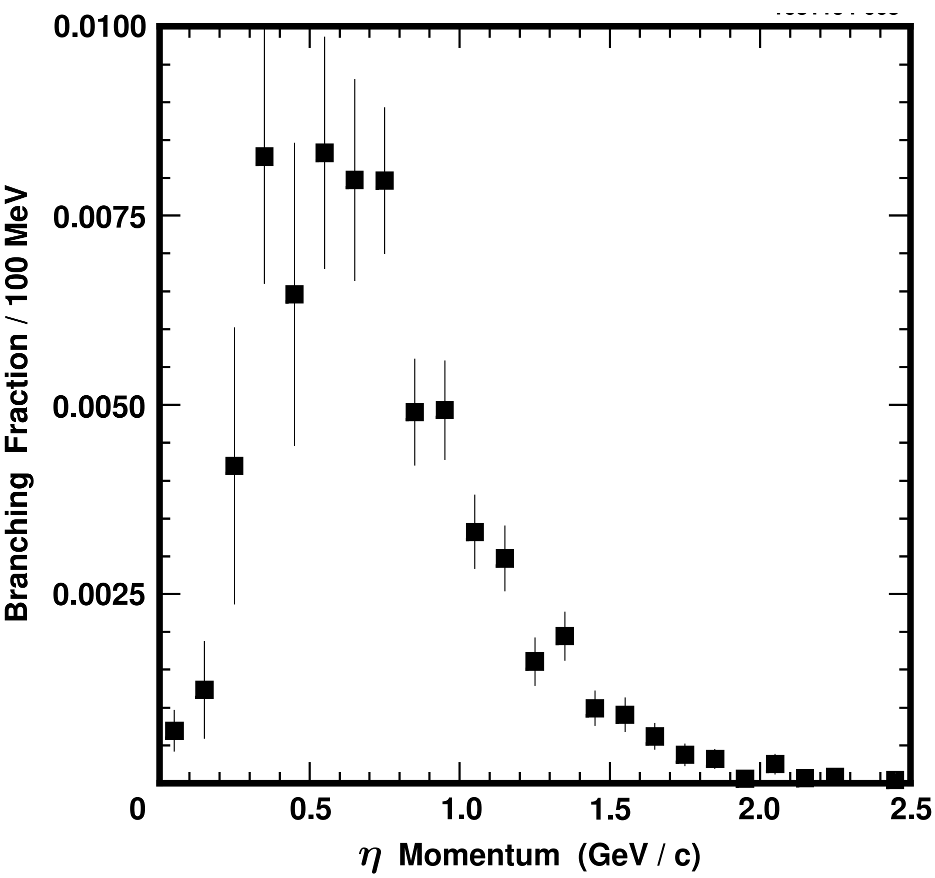

FIG. 5. Measured η momentum spectrum from B decay.